

# Behavior of Retaining Wall Nearby Machine Foundation in Sandy Soil

Noor Ali Thamer<sup>1</sup> , Safa Hussain Abd Awn<sup>1\*</sup> 

<sup>1</sup>Department for Civil Engineering, University for Diyala, Diyala, Iraq

## Abstract

This study experimentally investigates the frequency-dependent dynamic soil-structure interaction response for a retaining wall resting on sandy soil and a focus on identifying critical behavioral regimes under varying excitation frequencies. Controlled vibration tests were conducted at 10 Hz, 15 Hz, and 20 Hz in order to study the characteristics of vibration velocity, acceleration, displacement amplitude and settlement. The results show that when frequency increases, the response of elastic stability for progressive failure tends to decrease. At 10 Hz, the base exhibited stable elastic behavior and minor deformation. This meant it was operating safely. The places where the observations were made suggest that at the frequency of 15 Hz, the lateral dislocation ratio is more than 1.0. So, we conclude that plastic deformation happened. We also see the maximal dynamic response and vibration speed (1.23-4.61 mm/s) and acceleration (1.1-3.8 m/s<sup>2</sup>). The system experienced extreme compounded damage and settled nearly -20mm. Cyclic stress concentration and densification of soil also cause a large degree of lateral spreading. The results indicate a critical resonance (15 Hz) beyond which the dynamic instability builds up and design measures should be taken into consideration in terms of resonant amplification and long-term cyclic degradation to secure foundation safety and serviceability on vibrations caused by machines.

**Keywords:** Dynamic SSI; Retaining Wall; Vibrational Loading; Frequency; Sandy Soil.

*Article history: Received: 21 Jan. 2026, Accepted: 20 Feb. 2026, Published: 20 March 2026*

This article is open-access under the CC BY 4.0 license (<http://creativecommons.org/licenses/by/4.0/>).

## 1. Introduction

Retaining walls are useful geotechnical structures many times used in civil engineering for resisting lateral earth pressures under applications like highways, basements, bridge abutments and waterfront facilities [1]. In many real-world scenarios, retaining walls are exposed to continuous or intermittent dynamic loads [2]. The loads are generally created by machinery, traffic or nearby construction works, which can induce cumulative deformation and consequently affect the wall serviceability in long run [3]. It is essential to understand the dynamic response of retaining walls in order to achieve more resilient and durable retaining systems that deal with sandy soils [4].

Some studies examined the dynamic reaction of retaining walls that were given a wide variety of soil conditions and loadings. The early experimental research examined the use of tire-derived aggregates (TDA) as backfill. In this context, Hartman et al. [5] used shaking table tests to show reduced seismic earth pressures. This was confirmed later by Dammala et al. [6] and Reddy & Krishna [7], who showed TDA mixtures could effectively improve the seismic performance of retaining walls.

Yaghouti and Hajjalilu [8] focus on the effect of liquefiable backfills for a static routine wall design. They emphasize the need to consider static and dynamic effects. Researchers Haeri and Fathi used finite element techniques to show that controlled rocking can improve the performance of systems [9]. In another instance, Karami et al. provided analytical insights into the behavior of retaining walls subjected to transient pressure waves [10].

More factors have been investigated in analysis and numerical studies lately. Giwangkaraand et al. [11] found that internal friction angle, slope of the foundation, and the cohesion of backfill influence the ultimate stress. Allawi and Mohammed [12] studied the behavior of retaining walls to machine foundation loads using numerical simulations, while Abdul-Hussain et al. [13] researched the effect for blast loads on reinforced concrete walls and sand backfill. Chen et al. [14] did numerical analyses at ABAQUS and PLAXIS 2D. By Yavan et al [15], which provided safety assessment for walls at saturated clay and water-saturated sand under earthquake excitations. So, the soil saturation and wall height have a role to play. Guan and Madabhushi[16] evaluated walls and structures on dry

\* Corresponding author: [dr.safaalshamary@gmail.com](mailto:dr.safaalshamary@gmail.com)

backfill with centrifuge testing and dynamic displacement patterns through the tests.

Liu et al. [17] studied the approach of addressing fine-scale behavior with the aid of experimental studies. This study shows the beneficial effect of synthetic fibrous materials on sandy soil dynamic. Mazni et al. [18] studied the sand grain movement behind the retaining wall under static loads. Fattah et al. [19] used experimental approaches to trace lateral displacements for walls subjected to dynamic loading. Hassan and Zakaria [20] examined the settlement pattern in sandy backfill using numerical modeling. Zou et al [21]. evaluated the maximum impact energy of pile-slab retaining walls in their study.

According to recent investigations by El-Emam et al. [22] and Jaro and Mohammed [23], the transient and residual dynamic response of non-yielding walls supporting over-consolidated sand have been studied. The authors determined the dynamic stiffness and damping under dimensionless frequencies, respectively. Ren [24] looked for the deformation and bearing features for the sandy soil in the neighbourhood of the bucket foundations on an experimental basis.

Even though much progress has been achieved, well-controlled laboratory-scale studies must be designed to experimentally measure wall displacements, wall accelerations, and wall velocity response under precisely defined dynamic excitation frequencies and soil conditions.

This study investigates the dynamic behaviour of a concrete retaining wall embedded in sandy soil using controlled vibration loading tests conducted in a laboratory. The researchers in the experiment aimed to measure the horizontal and vertical displacements. Further, those displacements, and the velocity and acceleration of the wall are under 10, 15 and 20 Hz excitation frequencies. Similarly, the wall lasted in these frequencies for 30 continuous minutes and 65% relative soil density. This research intends to present insight on the temporal deformation behaviour and energy transmission characteristics of retaining walls under practical vibration conditions.

## 2. Materials and Methods

This section outlines the materials, equipment and procedures used for investigate the dynamic behavior for a retaining wall–soil system under controlled vibration loading. It covers the specifications for the retaining wall, physical and mechanical properties for the sandy soil, details for the experimental setup and the step-by-step testing procedures adopted for ensure accuracy and repeatability for results.

### 2.1 Soil Properties

The soil used at this study is a clean, uniformly graded sandy soil imported of Karbala Governorate, Iraq, classified as poorly graded sand according for the Unified Soil Classification System (USCS). Particle size distribution is determined via sieve analysis following

ASTM D422-63 (2006) and  $D_{10} = 0.18$  mm,  $D_{30} = 0.30$  mm,  $D_{50} = 0.41$  mm and  $D_{60} = 0.47$  mm, indicating uniform coarse sand (Fig. 1), while the key geotechnical properties for the soil are summarized at Table (1).

### 2.2 Retaining Wall Specifications

In this study, a gravity-type retaining wall is designed and constructed for fit within the laboratory container, ensuring proper placement and ease for handling during dynamic testing. The wall is fabricated using an iron mold and a wall thickness for 20 mm, height for 300 mm and width for 480 mm, which is approximately 20 mm smaller than the container width for allow for easy installation and removal. The mold dimensions are 500 mm length  $\times$  480 mm width  $\times$  320 mm height, providing sufficient allowance for concrete placement and demolding. The wall is reinforced using 4 mm diameter steel bars for ensure structural integrity during handling and testing, as presented at Fig. 2 (a).

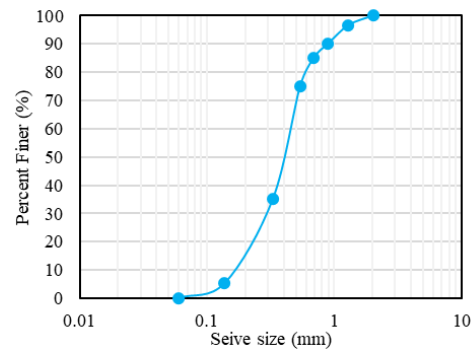


Fig. 1 Grain size distribution curve for the sandy soil

Table 1: Geotechnical properties for selected sandy soil

Property	Value	Standard
$D_{10}$ (mm)	0.18	ASTM D2487 (2006)
$D_{30}$ (mm)	0.3	ASTM D422 (2006)
$D_{50}$ (mm)	0.41	ASTM D422 (2006)
$D_{60}$ (mm)	0.47	ASTM D422 (2006)
Cu	2.6	ASTM D422 (2006)
Cc	1.1	ASTM D422 (2006)
USCS Class.	SP	ASTM D2487 (2006)
Gs	2.67	ASTM D854 (2006)
$\phi$ (°)	36-34	ASTM D3040 (2006)
c (kPa)	0	ASTM D3040 (2006)
$\gamma_{d_{max}}$ (kN/m <sup>3</sup> )	17.7	ASTM D4253 (2006)
$\gamma_{d_{min}}$ (kN/m <sup>3</sup> )	14.9	ASTM D4254 (2006)
$e_{max}$	0.8	ASTM D4254 (2006)
$e_{min}$	0.5	ASTM D4254 (2006)
$\gamma_d$ (kN/m <sup>3</sup> )	16.6	ASTM D4254 (2006)

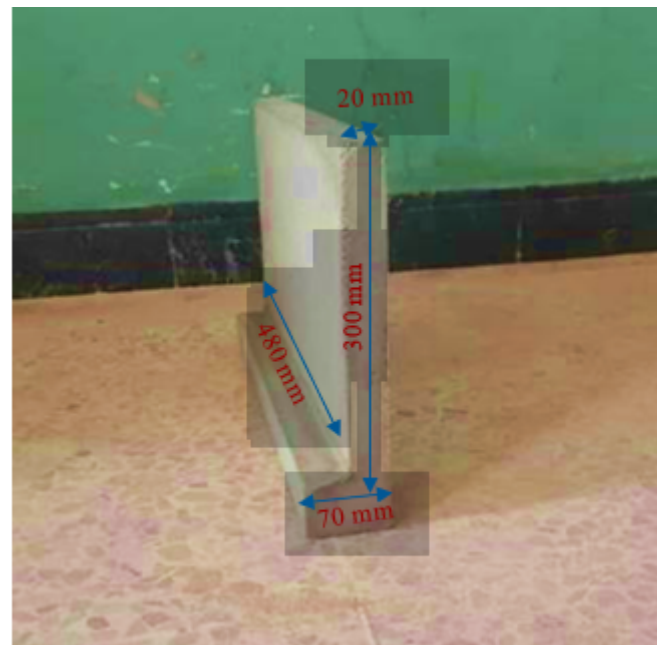
$D_r$ (%)	65	ASTM D4254 (2006)
-----------	----	-------------------

The concrete mix used for casting the wall followed a 1:1.8:2 ratios for cement, sand and gravel, respectively. The mix was chosen because it is a typical laboratory concrete that would be used to scale model retaining walls. The compressive strength of the mix after 28 days is about 32MPa and this value is added to the manuscript. Ordinary Portland cement is employed, while the sand is sourced from Karbala, Iraq and thoroughly washed to remove impurities and salts. Gravel and diameters ranging from 5 to 12 mm are obtained of the Construction Laboratory for the Civil Engineering Department at the University of Diyala. The mixing process is performed manually to

ensure uniformity. The mold is lubricated internally and a grease-based substance to facilitate demolding. Steel reinforcement is positioned within the mold before pouring the concrete. The concrete is added gradually and continuous stirring for remove air bubbles and ensure proper compaction. After casting, the mold is left for cure under ambient conditions: 28 days during winter and 14 days during summer. Following initial curing, the wall is demolded and submerged in water for 7-10 days to achieve complete hydration and the desired strength. The fully cured wall is then transferred to the soil laboratory for further experimental testing under controlled dynamic loading conditions (Fig. 2, b).



(a)



(b)

**Fig. 2** Current study retaining wall fabrication process.

(a) Reinforcement placement within the wall mold.

(b) Dimensions and layout

### 2.3 Experimental Setup

The experimental program is conducted at a rectangular steel container and three steel sides and a front side for reinforced glass, measuring 850 mm at length, 500 mm at width and 600 mm at height, coated and anti-corrosion paint. The container is placed on a base measuring 1430 × 670 mm.

Sandy soil and a relative density for 65% is leveled inside the container using a raining technique, presented at Fig. 3, which ensured uniform compaction and homogeneous layering. The retaining wall is positioned on a 300 mm sand layer, maintaining a 150 mm (0.5H) distance.



**Fig 3.** The raining technique device

The main equipment and devices employed at the experimental program included: the mechanical oscillator, vibration meter, digital tachometer, steel container, LVDTs, electronic dial gauges, static load apparatus, variable frequency drive, container stand and retaining wall. This integrated setup allowed precise measurement for horizontal and vertical displacements, velocity, acceleration and dynamic earth pressures under controlled vibrational loading conditions.

#### 2.4 Test Procedures

The experimental program is designed to systematically investigate the dynamic response of the retaining wall-soil system under controlled vibration loading. The source of vibration during the vertical excitation tests was a mechanical oscillator on a 100 x 100 mm steel standing, as presented in Fig. 4. The square footing was made of 5 mm thick steel, which has enough rigidity to act as a rigid footing in case of dynamic loading. The oscillator had a rotating disc of 60 mm diameter and 5 mm thick, which was made of steel, and a small eccentric mass (me) which was attached at an eccentricity of 20 mm about the rotational axis. One eccentric configuration that was 55 g was applicable in the entire study following the calibration of the machine foundation. The motor foundation was placed 150 mm off the retaining wall to identify the effects of soil and structure interaction so that it would be possible to measure the lateral movement.

Dynamic excitation is applied using a mechanical oscillator generating vertical vibrations at frequencies for 10, 15 and 20 Hz, each maintained for 30 minutes. These frequencies are the working frequency range of small-to-medium electric mechanical oscillators and are the normal spectrum of industrial machine foundations (10Hz and 20Hz). 15 Hz is the preliminary natural/resonant frequency range of the system due to initial calibration experiments. The vibration amplitude is adjusted by varying the eccentricity of the rotating mass. System frequency and velocity are verified throughout the tests using a digital tachometer (DT-2234C) for ensure stable operation.

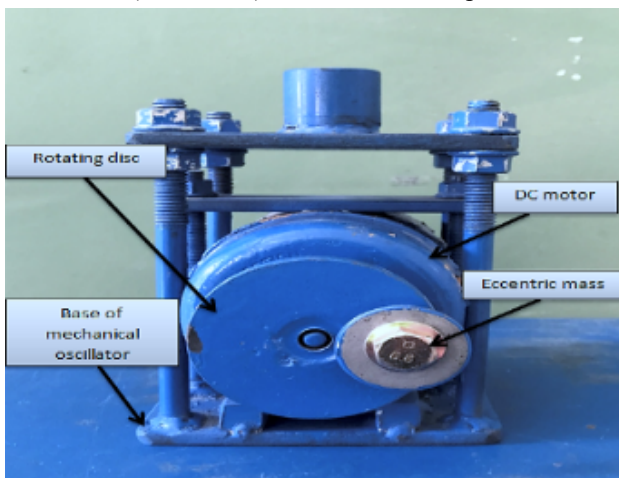


**Fig. 4** Mechanical oscillator device for vibration generation

The retaining wall and soil responses are monitored using several instruments: Linear Variable Differential Transformers (LVDTs) for record horizontal and vertical displacements, a vibration meter (HG 6360) for measure displacement, velocity and acceleration.

Prior to each test, the container is cleaned to remove left over soil. The sandy soil is prepared for 65% relative density using the raining method in order to maintain uniformity in the compaction. The retaining wall model is now kept on the precompacted sand layer inside the container. Before applying dynamic loading, they will record the baseline measurements, which include the wall alignment, sand surface elevation, and initial sensor readings.

The sand heaps in front and behind the retaining wall are intentionally imbalanced, 600 mm of sand behind the wall and 200 mm in front. It is a set-up that attempts to simulate an actual retaining-wall scenario in the real world whereby the backfill face is in increased lateral earth pressure mode and the front face has negligible passive resistance. The wall is therefore free to experience calculably lateral movement, rotating and settlement on dynamic loading. This unevenness of the soil distribution is highly fundamental in the appropriate determination of soil and wall interaction, lateral movement as well as deformation behavior under vibrating test.

During testing, vibration frequencies are applied sequentially for evaluate the response under increasing excitation levels. Real-time monitoring for displacement, velocity, acceleration and lateral soil pressure ensured precise tracking for the soil-wall interaction for each vibration phase. The final test setup can be visualized as presented in Fig. 5.



**Fig. 5** Laboratory container setup for the current study

### 3. Results and Discussion

The experimental results, presented in Fig. (6 a - d) obtained at vibration frequencies for 10 Hz, 15 Hz and 20

Hz illustrate a clear frequency-dependent behavior for the soil-foundation system at terms for velocity, acceleration, displacement amplitude and settlement.

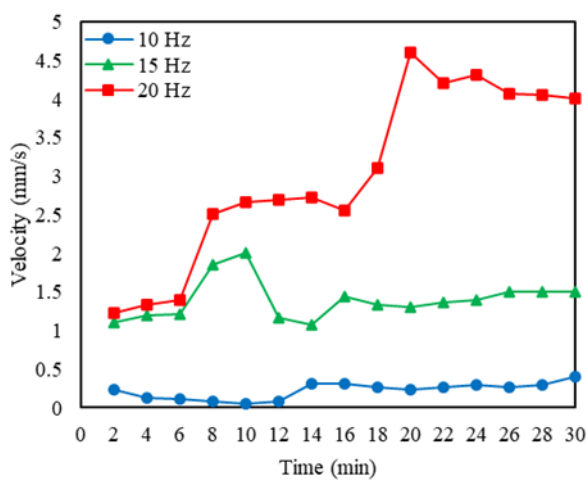
The vibration response is weak at 10 Hz with a frequency of 0.06-0.41 mm/s and this means that the energy transfer to the soil mass is low and will not cause much disturbance to the soil mass. The resulting acceleration ranged between 0.11 and 1.1 m/s<sup>2</sup> which is indicative of small oscillations and largely elastic soil action. The amplitude of the displacement was kept at the lower level (0.010021 mm), which led to the small deformations and minimal strain energy. First, the settlement rose slowly between -0.011 mm and -0.231 mm in 30 minutes, which was progressive as a result of light cyclic compressions. The 10 Hz reaction as a whole show that it is an elastic and stable system and has negligible permanent deformation and low energy dissipation.

The dynamic response at 15 Hz frequency is clearly amplified which is an indication of closeness of natural frequency. The speed values went from 1.07 to 2.01 mm/s implying energy and wall-soil interaction.

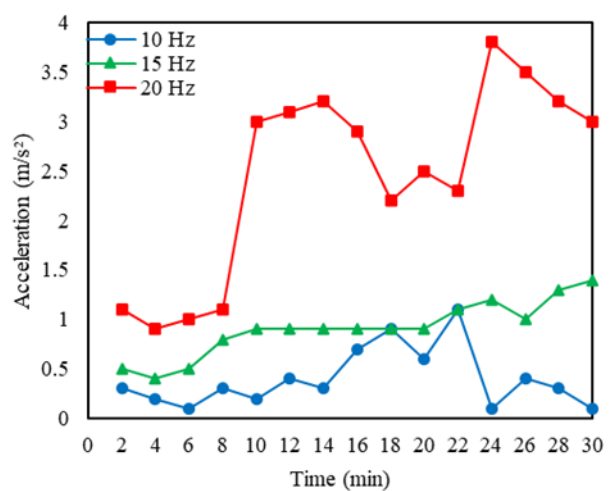
The retaining wall-soil interaction showed an amplified velocity response as the loading was increased; but, localized misalignment of particles and a slippage of the grains lowered the efficiency of soil-structure energy transfer. When the system reached this phase, the acceleration was measured to rise to 1.4 m/s<sup>2</sup>, with more dynamic stresses occurring, which facilitated rearrangement of particles in the sandy soil matrix. The rate of settlement was rather rapid, with the corresponding displacement amplitudes (0.032 -0.069 mm) being relatively small, but the settlement rate was reaching -12.13 mm at a rate of -0.015 mm/s. This is an indication of the beginning of plastic deformation with eventual physical densification of the soil. This regime witnessed resonant amplification which is maximum energy transmission and greater deformation of the soil and the structure.

When the frequency was increased to 20 Hz, the system shifted to a highly dynamic but partially damped response. Vibration velocity also rose to 1.23-4.61 mm/s, acceleration rose to 1.1-3.8 m/s<sup>2</sup>, which means that the cyclic input was higher, and the energy transfer remained a permanent increment. Although this acceleration was considerable, movements of the displacement were also small, between 0.054 and 0.078 mm. Such attenuation of the displacement at higher frequencies is in line with the negative relationship between the amplitude and the angular frequency in dynamic-loaded system. The greatest finding at 20 Hz was the cumulative accumulation of settlement, which was continuous and increasing at an accelerated rate; the settlement decreasing between -7.89mm to up to -20.4mm. These high vertical strains imply extreme cyclic densification and the possibility of soil fracture as a result of extended high-frequency vibration. This is a cumulative degradation which points out the vulnerability of the sandy soils to instability during compaction due to continuous loading of high frequency dynamics.

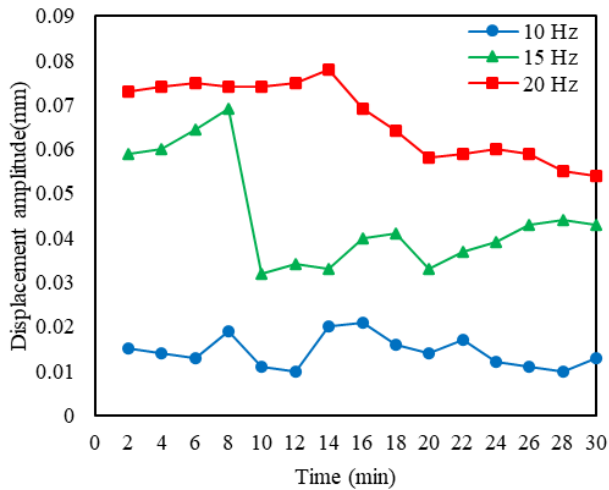
In summary, the answer of system gets considerably cube as the increasing excitation frequency. At a frequency of 10 Hz, the behavior remains predominantly elastic, stable, and with minimal deformation and limited energy transfer through the soil mass encapsulation. As the frequency increases for 15 Hz, the system signifies resonant amplification by peak energy transfer that produces greater vibration amplitudes and a conversion from elastic to plastic deformation. When the frequency is increased to 20Hz, the dynamic response shows high non-linearity due to cyclic stresses and permanent settlement occurring, which indicate the extent of soil compaction and stiffness degradation. All in all, the results indicate that 15 Hz corresponds for the near-resonant frequency for the wall-soil system, which is where dynamic effects are maximized, whereas 20 Hz induces the largest permanent deformation due for more intensified cyclic loading and cumulative soil densification.



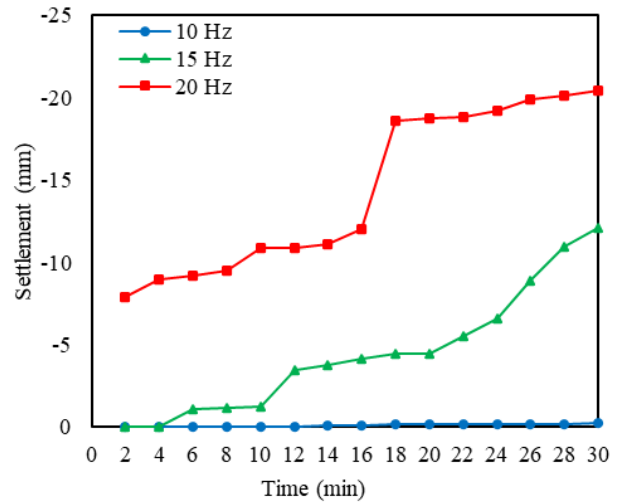
(a) Velocity (mm/s).



(b) Acceleration (m/s²).

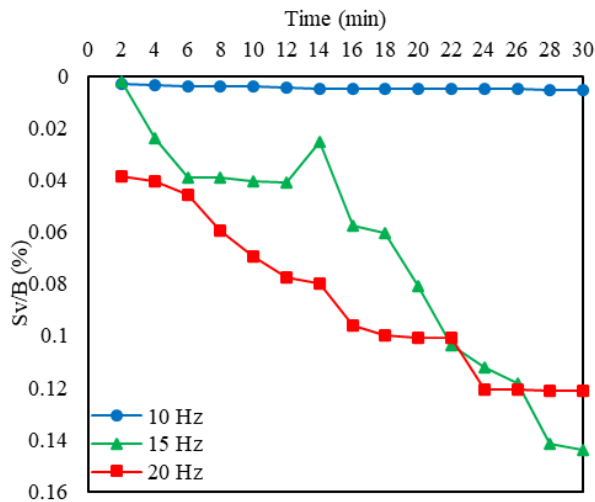


(c) Displacement amplitude (mm).

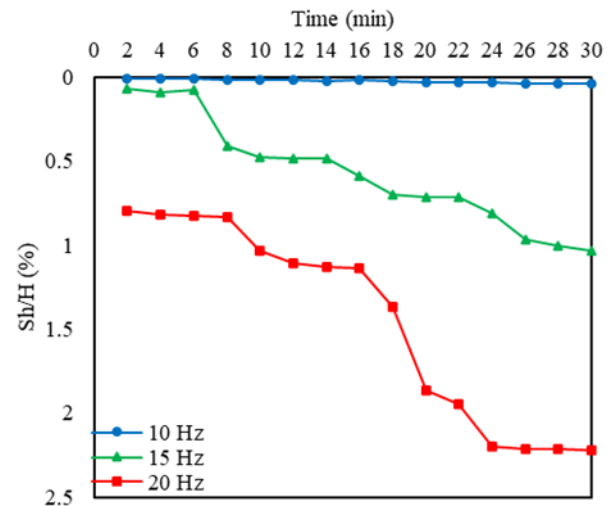


(d) Settlement (mm).

Fig. 6 Comparative results for dynamic response parameters for machine footing



(a) Vertical displacement (Sv/H).



(b) Lateral displacement (Sh/H)

Fig. 7. Normalized displacement for the retaining wall at different excitation frequencies

The normalized outcomes of Sv/B and Sh/H, Sv is the vertical displacement (settlement) and Sh is the horizontal displacement (lateral movement or rotation), at different excitation levels (10, 15 and 20 Hz) clearly demonstrate the frequency-dependent behavior for the retaining wall-soil system, as illustrated at (7, a and b).

The Sv/B and Sh/H values are low (approximately  $\leq 0.005$  and  $\leq 0.04$ ) at 10 Hz, indicating a stable and elastic response. The slow and almost straight increase of both ratio and time indicates that deformation is limited, soil has penetrated little and not lateral displacement. It shows a condition of equilibrium where soil and wall deformations take place elastically at low dynamic excitation.

The normalized displacements are much greater at 15 Hz. The increase of Sv/B r is estimated at 0.144 of 0.00175 and of Sh/H is drastic with an increase of over 1.03 of

0.065 in 30 seconds. This act is near resonance; lateral movement is highly enhanced by cyclical loading as opposed to vertical settlement. Lateral displacement and rotation of the wall at Sh/H is the major factor that causes the pattern of deformation.

The deformation is significantly increased and extremely nonlinear at 20 Hz The Sv/B ratio increased by 0.12 and the Sh/H value exceeded 2.2, indicating the most robust dynamic amplification among all cases. As the wall displaces horizontally and settles more, it damages the wall permanently. Change in the sample location and thickness is the cause of natural frequencies above 10Hz.

Deformation is highly influenced by frequency, as per results. The system is elastic and stable at 10 Hz. At 15 Hz, resonance magnifies movements cyclic causing plastic behaviour. At 20 Hz, very large cyclic loading leads to

major plastic deformation. As such, 15 Hz is the resonant frequency and 20 Hz leads to progressive instability.

These experimental tendencies are generally consistent with previous experimental and numerical studies: Hamdi et al. [25] had shown more settlement and lateral displacement when the amplitude of the load was higher or the source was more proximate, as with our larger  $Sh/H$  and cumulative settlement at 15-20 Hz. Numerical analysis by Hassan and Zakaria [20] also demonstrates that machine-type excitations around a wall may enhance horizontal movements by an order of magnitude and analytical computations by Jaro and Mohammed [23] reveal that stiffness and damping are strongly frequency dependent, a phenomenon that is likely to explain why the amplitude of displacements reduced, but settlements increased as tests were conducted. New confirmed simulations and experiments by El-Emam et al. [22] and Ren [24] also support this fact, that resonant conditions result in maximal dynamic response and that exposure to higher frequencies aggravates cumulative and usually irreversible deformations. The difference between the absolute magnitudes is identified to be due to scale, input amplitude, length of test and boundary effects; therefore, it is better to compare them using nondimensional measures (e.g.,  $S/B$ ,  $Sh/H$ ,  $ao$ ).

#### 4. Conclusion

In the current research, the excitation frequency effect on dynamic response of a machine foundation on reinforced sandy soil was studied, and it revealed the three different performance regimes, which are dependent on frequency change.

The findings illustrate that the performance capacity of the system is subjected to progressive failure processes. The foundation at 10 Hz excitation frequency showed a highly elastic behavior with negligible displacements meaning that the operation was in a safe zone where the transfer of energy is low and the structural response is stable.

The resonant frequency of the system was found to be 15 Hz with large amplification in the velocity of vibrations (1.23-4.61 mm/s) and acceleration (1.1-3.8 m/s<sup>2</sup>). At this regime, plastic deformation began because the ratio of the normalized lateral displacement ( $Sh/H$ ) was greater than unity, which indicated the beginning of the serious lateral movement.

At a frequency of 20 Hz, the system experienced cumulative degradation in its severe forms, with settlements reaching up to -20 mm and ratio of lateral displacement up to 2.2 as this is a sign of excessive densification of soil, spreading laterally, and diminishing its stiffness. Whereas the damping of the soil slightly reduced the amplification of dynamic response, cyclic stresses accumulation controlled the response, and progressive instability was achieved.

Engineering In these results, one can highlight the rule that safe design of a dynamic object must be based not only on avoiding resonance but also on the fact that resonance-induced amplification and cumulative damage of high-frequency cyclic loading should also be taken into

consideration during its design to support the safety and stability of machine foundations.

#### Conflict of interest

The authors declare that there are no conflicts of interest regarding the publication of this manuscript.

#### References

- [1] Ajayi, O., Okeke, O. C., Okonkwo, S. I., & Amadi, V. F. C. (2023). Analysis for Earth Pressures and Stability for Retaining Walls; Review for Principles and Practices at Eng. Construction. *Int. J. Eng. Mod. Technol*, 9(1), 42-57.
- [2] Putra, P. R., Oetomo, W., & Marleno, R. (2025). Technical and Economic Feasibility Study for Retaining Wall Construction on the Temuireng Road Section at Mojokerto District. *Asian Journal for Eng., Social and Health*, 4(4).
- [3] Han, J., Jiang, Y., & Xu, C. (2018). Recent advances at geosynthetic-reinforced retaining walls for highway applications. *Frontiers for Structural and Civil Engineering*, 12(2), 239-247.
- [4] Johari, A., & Elyasi, H. (2024). Analytical system reliability analysis for a geotextile-reinforced retaining wall. *International Journal for Geomechanics*, 24(10), 04024231.
- [5] Hartman, D., Ledezma, M., Xiao, M., & Zoghi, M. (2013). Shake table test for MSE wall and tire derived aggregates backfill. at *Geo-Congress 2013: Stability and Performance for Slopes and Embankments III* (pp. 1168-1177).
- [6] Dammala, P. K., Sodom, B. R., & Adapa, M. K. (2015). Experimental investigation for applicability for sand tire chip mixtures as retaining wall backfill. at *IFCEE 2015* (pp. 1420-1429).
- [7] Reddy, S. B., & Krishna, A. M. (2015). Recycled tire chips mixed and sand as lightweight backfill material at retaining wall applications: an experimental investigation. *International Journal for Geosynthetics and Ground Engineering*, 1(4), 31.
- [8] Yaghouti L. A., & Hajjalilu B. M. (2018). Investigation into Effect for Liquefaction on Behavior for Retaining Wall. *Journal for Civil Engineering and Materials Application*, 2(4), 201-215.
- [9] Haeri, S. M., & Fathi, A. (2018). Numerical modeling for rocking for shallow foundations subjected for slow cyclic loading and consideration for soil-structure interaction. *arXiv preprint arXiv:1808.04492*.
- [10] Giwangkara, G. G., Mohamed, A., Nor, H. M., & Mudiyo, R. (2020). Analysis for internal friction angle and cohesion value for road base materials at a specified gradation. *JACEE (Journal for Advanced Civil and Environmental Engineering)*, 3(2), 58-65.
- [11] Karami, M., Kabiri-Samani, A., Nazari-Sharabian, M., & Karakouzian, M. (2019). Investigating the effects for transient flow at concrete-lined pressure tunnels and developing a new analytical formula for

- pressure wave velocity. *Tunnelling and Underground Space Technology*, 91, 102992.
- [12] Allawi, A. A., & Mohammed, Q. S. (2022). Numerical analysis for a concrete foundation under a combination for a dynamic and a seismic load. *Journal for Engineering*, 28(2), 18-39.
- [13] Abdul-Hussain, N., Fall, M., & Saatcioglu, M. (2022). Blast induced lateral earth pressures on retaining structures and sand backfill. *International Journal for Impact Engineering*, 166, 104253.
- [14] Chen, C., Wang, Y., Zhang, X., Kong, L., & Xu, G. (2022). Numerical modelling for gassy sand behaviour under monotonic loading. *Acta Geotechnica*, 17(5), 1667-1680.
- [15] Yavan, O., Tabak, T., & Tuncan, A. (2022). Behavior for retaining walls constructed at the saturated clay and water-saturated sand soils under the dynamic loads. *Kirklareli University Journal for Engineering and Science*, 8(2), 253-272.
- [16] Guan, X., & Madabhushi, G. S. (2022). Dynamic response for a retaining wall and a structure on the dry backfill. *Soil Dynamics and Earthquake Engineering*, 157, 107259.
- [17] Liu, L., Zhao, J., Liu, X., & Lv, S. (2023). Dynamic characteristics and reinforcement mechanism for silty soil improved by regenerated fiber polymer. *Scientific Reports*, 13(1), 18219.
- [18] Mazni, D. I., Hakam, A., Tanjung, J., & Ismail, F. A. (2023). Failure plane on precast block retaining wall. *Civil and Environmental Engineering*, 19(1), 86-94.
- [19] Fattah, M. Y., Hussein, H. H., Aswad, M. F., & Hamdi, R. E. (2024). Studying the lateral displacement for retaining wall supporting sandy soil under dynamic loads. *Open Engineering*, 14(1), 20220553.
- [20] Hassan, F. M., & Zakraia, W. A. (2024). Numerical Study for Soil-Retaining Wall Behavior Subject for Machine Foundations Loads. *Diyala Journal for Engineering Sciences*, 91-100.
- [21] Zou, P., Luo, G., Bi, Y., & Xu, H. (2024). Dynamic response for pile-slab retaining wall structure under rockfall impact. *Natural Hazards and Earth System Sciences*, 24(10), 3497-3517.
- [22] El-Emam, M., Bigdeli, A., El Berizi, Y., & Tabsh, S. W. (2025). Dynamic Response for Non-Yielding Wall Supporting Over-Consolidated Sand. *Applied Sciences*, 15(11), 6131.
- [23] Jaro, M. N., & Mohammed, A. I. (2025). Dynamic Stiffness and Damping for Rigid Retaining Wall under Seismic Loading. *Tikrit Journal for Engineering Sciences*, 32(3), 1-12.
- [24] Ren, M. (2025). Experimental study on deformation for sandy soil around bucket foundation under horizontal load. *Scientific Reports*, 15(1), 12803.
- [25] Hamdi, R. E., Fattah, M. Y., & Aswad, M. Y. (2020). Studying the settlement of backfill sandy soil behind retaining wall under dynamic loads. *Eng. Technol. J*, 38, 992-1000.